JOURNAL OF VIROLOGY, June 2011, p. 5446–5455 Vol. 85, No. 11
0022-538X/11/$12.00 doi:10.1128/JVI.02611-10

Pivotal Role of Antibody and Subsidiary Contribution of CD8$^+$ T Cells to Recovery from Infection in a Murine Model of Japanese Encephalitis$^\nabla$

Maximilian Larena, Matthias Regner, Eva Lee, and Mario Lobigs*

John Curtin School of Medical Research, The Australian National University, Canberra, ACT, Australia

Received 15 December 2010/Accepted 21 March 2011

The immunological correlates for recovery from primary Japanese encephalitis virus (JEV) infection in humans and experimental animals remain poorly defined. To investigate the relative importance of the adaptive immune responses, we have established a mouse model for Japanese encephalitis in which a low-dose virus inoculum was administered into the footpads of adult C57BL/6 mice. In this model, ~60% of the mice developed a fatal encephalitis and a virus burden in the central nervous system (CNS). Using mice lacking B cells ($\mu MT^{-/-}$ mice) and immune B cell transfer to wild-type mice, we show a critically important role for humoral immunity in preventing virus spread to the CNS. T cell help played an essential part in the maintenance of an effective antibody response necessary to combat the infection, since mice lacking major histocompatibility complex class II showed truncated IgM and blunted IgG responses and uniformly high lethality. JEV infection resulted in extensive CD8$^+$ T cell activation, judged by upregulation of surface markers CD69 and CD25 and cytokine production after stimulation with a JEV NS4B protein-derived H-2D^b-binding peptide and trafficking of virus-immune CD8$^+$ T cells into the CNS. However, no significant effect of CD8$^+$ T cells on the survival phenotype was found, which was corroborated in knockout mice lacking key effector molecules (Fas receptor, perforin, or granzymes) of cytolytic pathways triggered by T lymphocytes. Accordingly, CD8$^+$ T cells are mostly dispensable for recovery from infection with JEV. This finding highlights the conflicting role that CD8$^+$ T cells play in the pathogenesis of JEV and closely related encephalitic flaviviruses such as West Nile virus.

Japanese encephalitis virus (JEV) is a mosquito-borne flavivirus belonging to the JEV serocomplex, which also includes the closely related viruses Murray Valley encephalitis virus (MVEV) and West Nile virus (WNV). In terms of the incidence and severity of disease in humans, JEV is the most important member of this serocomplex. It is the leading cause of viral encephalitis in Asia, accounting for 35,000 to 50,000 cases per year and an estimated 10,000 deaths, with long-term neurologic sequelae in about one-half of the survivors (43). In the past decades, there has been an expansion of the geographic distribution of the virus in Asia and emergence of virus transmission and human cases of encephalitis in Pakistan, the eastern Indonesian archipelago, New Guinea, and northern Australia (reviewed in reference 28). Vaccination is the main measure for protection against Japanese encephalitis (reviewed in reference 3), but due to expense and logistics, it is not available to a large population in Asia that should be immunized.

The majority of human infections with JEV are subclinical, with the ratio of apparent to inapparent infections estimated to range from 1:25 to 1:1,000 (43). Host factors, rather than variation in viral virulence, are thought to dominantly determine the outcome of infection in terms of disease severity (reviewed in reference 15). Of these factors, an understanding of the immunological responses that lead to recovery from JEV infection is important for the design of rational approaches to new treatments and vaccines. However, insight into the immunological correlates of recovery from JEV infection is incomplete (reviewed in reference 31). Among the innate immune pathways, an essential role for type I interferons (IFN) in recovery is illustrated by the uncontrolled growth of the virus in mice lacking a functional IFN-α receptor (22). Similarly, the importance of a vigorous humoral immune response in ameliorating or preventing illness has been documented in human cases of Japanese encephalitis (6, 23) and in animal models by administration of antibody prior or subsequent to infection with JEV (13, 14, 18, 48). In contrast, the relative contribution of cellular immune responses to recovery from JEV infection remains unclear. A limited number of studies with mice suggest, for instance, a protective value of JEV-immune CD4$^+$ T cells by a mechanism involving enhanced antibody production (4) and a possible role for CD8$^+$ T cells in virus clearance (33), although the latter study involved the coinjection of a large number of splenocytes with virus into the brain and required cotransfer of CD4$^+$ T cells. Thus, insight into the immunobiology of JEV is lagging in comparison to the significantly more detailed understanding of the role of innate and adaptive immune responses in recovery from infection with the related virus WNV, predominantly derived from studies on virulent lineage I North American isolates in mice deficient in defined immune effector functions (reviewed in reference 20). This raises the question of the generality of immunological correlates identified for WNV as

* Corresponding author. Mailing address: Department of Emerging Pathogens and Vaccines, John Curtin School of Medical Research, The Australian National University. P.O. Box 334, ACT 2600, Australia. Phone: 61 2 61254048. Fax: 61 2 61252595. E-mail: Mario.Lobigs@anu.edu.au.

$^\nabla$ Published ahead of print on 30 March 2011.

determinants of disease outcome for JEV and other viruses of medical importance belonging to the JEV serocomplex (32). For instance, the contribution of $CD8^+$ T cells to recovery from flaviviral infection is variable and can range from protective to immunopathological outcomes (24, 38, 46). To begin to answer this question, we have established a pathogenesis model with adult C57BL/6 (B/6) mice for Japanese encephalitis involving conditions that mimic the natural infection route and dose and report both commonalities with and differences from WNV in the role of adaptive immune pathways in recovery from JEV infection.

MATERIALS AND METHODS

Virus and cells. Working stocks of JEV (strain Nakayama) were infected Vero cell culture supernatants (2×10^8 PFU/ml) stored in single-use aliquots at −70°C. Vero cells were grown at 37°C in Eagle's minimal essential medium plus nonessential amino acids (MEM) supplemented with 5% fetal calf serum (FCS). Virus titration was by plaque assay on Vero cell monolayers, as described for MVEV (24).

Mice. B/6, 129x1/SvJAPB (129), and B/6 congenic B cell-deficient ($\mu MT^{-/-}$) (19), major histocompatibility complex class II α and β chain-deficient ($MHCII^{-/-}$) (29), Fas receptor-deficient ($Fas^{-/-}$) (1), perforin-deficient ($perf^{-/-}$) (16), and granzyme A and B-deficient ($gzmA/B^{-/-}$) (41) mice were bred under specific-pathogen-free conditions and supplied by the Animal Breeding Facility at the John Curtin School of Medical Research, The Australian National University (ANU), Canberra. Female mice were used in all experiments. All animal experiments were conducted with approval from the ANU Animal Ethics Committee.

Mouse inoculation and tissue collection. Mice were anesthetized with 50 μl of a 10% ketamine–xylazole solution in phosphate-buffered saline (PBS) by intramuscular injection. Mice were infected subcutaneously (s.c.) via the footpad or intracranially (i.c.) with a single injection of a defined dose of JEV in 20 μl Hanks' balanced salt solution containing 20 mM HEPES (pH 8.0) and 0.2% bovine serum albumin (HBSS-BSA). Mice were monitored twice daily, and severely moribund mice were euthanized by cervical dislocation. For tissue processing, mice were euthanized at the time points indicated and a sterile midline vertical thoracoabdominal incision was made to expose the internal organs. After cardiac puncture for blood collection, animals were perfused with 10 ml sterile PBS. The brain was excised intact and dissected into samples for virus titration and histological study. For determination of virus titers, sample tissues were snap-frozen on dry ice. One-half of the brain samples were placed in cell culture medium and homogenized for lymphocyte isolation.

Real-time RT-PCR. For determination of viral burdens in mouse serum and spleen samples, the total RNA in 50 μl of splenic homogenates (10% [wt/vol]) and 50 μl of serum was extracted using Trizol (21), and virion RNA content, expressed in genome equivalents, was determined by quantitative reverse transcription (RT)-PCR. For a standard, JEV RNA extracted from a Vero cell-grown virus stock and quantitated by spectrophotometry was used. RT was performed at 43°C for 90 min in a 10-μl mixture containing 2 μl sample RNA, Expand reverse transcriptase (Roche), RNase inhibitor (Invitrogen), 10 mM deoxynucleoside triphosphate, 10 pmol downstream primer (5′-TTGACCGTT GTTACTGCAAGGC-3′), 10 mM dithiothreitol, and the manufacturer's recommended buffer condition. Real-time PCR was performed using IQSybr qPCR mixture (Bio-Rad) and 0.2 nM downstream and upstream primers (5′-GCTGG ATTCAACGAAAGCCACA-3′) under cycling conditions of 95°C for 3 min for 1 cycle and 95°C for 30 s, 63°C for 30 s and 72°C for 60 s for 40 cycles. Each sample was tested in duplicate, and genome copy numbers were determined by extrapolation from the standard curve generated within each experiment. The detection limit of the assay was 4×10^3 RNA copies/ml.

Histology and immunohistochemistry analysis. After dissection, brain tissue samples were placed in 10% neutral buffered formalin fixative and stored at room temperature. For examination of basic cell morphology and neuronal myelin integrity, 6-μm sagittal brain sections were stained with hematoxylin-eosin and luxol fast blue, respectively. Immunohistochemistry analysis was performed with an avidin-biotin complex technique. Triplicate sagittal sections of brain samples were incubated overnight with anti-NS1 monoclonal antibody 4G4 (9) at 4°C to stain JEV antigen. After 10 min of incubation at room temperature with biotinylated rabbit anti-rat Ig (Dako Corporation) as the secondary antibody, specimens were incubated for 10 min at room temperature with a streptavidin-horseradish peroxidase (HRP) complex (Dako Corporation). Subsequently, a mixture of 3,3′-diaminobenzidine tetrahydrochloride chromogen and substrate buffer (Dako Corporation) was applied for 5 min at room temperature. Slides were examined under bright-field microscopy, and brown staining of cells was indicative of positive immunoreactivity.

Lymphocyte isolation from the brain. Homogenized brain samples were digested with 2 mg/ml collagenase type I (Gibco-Life Technologies) in MEM plus 5% FCS for 45 min at 37°C with intermittent shaking and then centrifuged at $400 \times g$ for 10 min. Pellets were resuspended in 2 ml 90% Percoll in minimum essential medium (MEM) plus 5% FCS and overlaid gently with 60%, 40%, and 10% Percoll (GE Healthcare) in MEM plus 5% FCS. The gradients were centrifuged at $800 \times g$ for 45 min at 25°C, and lymphocytes were collected from the 40 to 60% interface were subsequently analyzed by flow cytometry.

Cell surface and intracellular cytokine staining. The surface marker staining employed in this study utilized the following reagents: allophycocyanin (APC)-conjugated anti-CD8 antibody; phycoerythrin (PE)-conjugated anti-CD3, anti-CD69, and anti-CD25 antibodies; fluorescein isothiocyanate (FITC)-conjugated anti-CD4 and anti-CD19 antibodies; and 7-aminoactinomycin D (all reagents from BD Biosciences). One hundred thousand events were acquired for each sample on a four-color FACSort flow cytometer. Results were analyzed using Cell Quest Pro Software. For intracellular cytokine staining, 1×10^6 spleen- or brain-derived lymphocytes were suspended in 100 μl MEM with 5% FCS and stimulated for 16 h with 10^{-4} M H-$2D^b$-binding 9-mer JEV E protein-derived (TAWRNRELL) or NS4B protein-derived peptide (SAVWNSTTA) in the presence of 1 μl/ml brefeldin A (eBioscience). An ectromelia virus (ECTV) K^b-restricted peptide, TSYKFESV (45), was used at 10^{-4} M as a negative-control peptide. For stimulation of *ex vivo* splenocytes with JEV, splenocytes were infected at a multiplicity of infection of 1 for 1 h at 37°C and washed twice with MEM plus 5% FCS before incubation for 16 h in MEM plus 5% FCS in the presence of brefeldin A. Cells were surface stained with anti-CD8–APC before paraformaldehyde fixation and permeabilization with saponin (Biosource) according to the supplier's instruction. Cells were then stained with anti-IFN-γ–FITC (BioLegend) and anti-tumor necrosis factor alpha (TNF-α)–PE (Invitrogen) and washed twice with fluorescence-activated cell sorter (FACS) washing buffer (2% FCS in PBS) before assessment by FACS analysis.

In vivo depletion of $CD8^+$ T cells. $CD8^+$ T cells in B/6 and 129 mice were depleted by intraperitoneal (i.p.) injection with 0.5 mg of a rat anti-mouse CD8a monoclonal antibody (2.43, IgG2b; BioXcell). Control mice were injected with 0.5 mg of an isotype control antibody (MPC-11, IgG2b; BioXcell). The antibodies were diluted in 0.5 ml PBS and injected at 3 days, 2 days, and 1 day before and 7 days after virus infection. The efficiency of depletion measured on day 7 postinfection (p.i.) was >98% based on FACS analysis of lymphocytes in blood.

Transfer experiments. Eight-week-old B/6 mice were infected with 1×10^3 PFU of JEV i.v. and sacrificed a week later for aseptic removal of spleens. Single-cell splenocyte suspensions were prepared by pressing the spleen tissue gently through a fine metal mesh tissue sieve. Erythrocyte lysis was by suspension of the splenocyte pellet in 4.5 ml distilled water, followed immediately by the addition of 0.5 ml of 10× PBS. Lysed cells were discarded after centrifugation at $400 \times g$ for 5 min. Splenocytes were resuspended in 100 μl PBS and injected through the lateral tail vein into 8-week-old B/6 recipient mice. Recipient mice were challenged a day later with 1×10^3 PFU JEV via footpad injection. For B cell depletion, splenocytes were incubated with anti-CD19 magnetic beads (Miltenyi Biotec) and loaded onto magnetic columns according to the supplier's instruction. Effluent from the columns was collected, and cells were pelleted by centrifugation at $400 \times g$ for 5 min. The efficiency of B cell depletion was >99% as assessed by FACS analysis. For further enrichment of either $CD4^+$ or $CD8^+$ T cells, B cell-depleted splenocytes were incubated with a 1:3 dilution of either anti-CD4 (RL4172) or anti-CD8 (31 M) supernatant in MEM plus 5% FCS for 30 min at 4°C, followed by incubation with rabbit serum complement (Cedarlane Laboratories) for 30 min at 37°C. Cells were washed twice with PBS before transfer into recipient mice. The efficiency of depletion of $CD4^+$ or $CD8^+$ cells was >95% as assessed by FACS.

Serological tests. For titration of JEV-specific antibody isotypes in mouse serum, ELISAs were performed with HRP-conjugated rabbit anti-mouse Ig and the peroxidase substrate 2,2′-azino-di(3-ethyl-benzthiazoline sulfonate). The JEV Nakayama strain was used for enzyme-linked immunosorbent assay (ELISA) antigen production as described for MVEV (10). For determination of ELISA endpoint titers, absorbance cutoff values were established as the mean absorbance of eight negative-control wells containing sera of naive mice plus 3 standard deviations (SD). Absorbance values of test sera were considered positive if they were equal to or greater than the absorbance cutoff, and endpoint titers were calculated as the reciprocal of the last dilution giving a positive absorbance value. Neutralization titers, measured in a 50% plaque reduction neutralization test, were determined as previously described (27).

TABLE 1. Effect of JEV dose on the mortality rates and survival times of B/6 mice

Challenge route and dose (no. of PFU)[a]	% Deaths (no. of deaths/total)	MST (days) ± SD	% Seroconversion of surviving mice[b]
Subcutaneous			
10	63 (5/8)	11.8 ± 1.1	100
10^2	67 (10/15)	12.8 ± 2.5	100
10^3	63 (12/19)	13.3 ± 1.7	100
10^5	60 (3/5)	9.7 ± 1.5	100
10^7	100 (5/5)	6.0 ± 0.7	
Intracranial			
0.1	0 (0/5)		60
1	80 (4/5)	10.3 ± 1.0	100
10	100 (5/5)	8.0 ± 1.4	
10^2	100 (5/5)	6.4 ± 0.5	

[a] Eight-week-old B/6 mice were infected with various doses of JEV via the s.c. or i.c. route. Virus doses in 20 μl HBSS-BSA are shown. Surviving mice were monitored for 28 days.

[b] Antibody against JEV in serum of surviving mice was measured at 28 days p.i. by ELISA.

Statistical analyses. Mortality data were plotted into Kaplan-Meier curves and assessed for significance by the log-rank test. The Mann-Whitney test was applied to assess differences between data gathered from two experimental groups. A P value of ≤ 0.05 was considered significant.

RESULTS

Mouse model of Japanese encephalitis by s.c. infection of adult B/6 mice with a low-dose virus inoculum. To establish a mouse model for Japanese encephalitis which resembles the natural infection route and virus dose and which allows investigation of the immunological correlates for recovery from infection, the pathogenesis of the prototype (Nakayama) strain in adult (8-week-old) B/6 mice was first characterized. After a low-dose s.c. challenge with 10^3 PFU of JEV, >50% of the infected mice showed clinical signs of infection starting at day 10 p.i., which included progressive generalized paresis, piloerection, and rigidity. Severe neurological impairment demonstrated by ataxia, postural imbalance, and generalized tonic-clonic seizures were evident later in the course of infection, invariably leading to death within 24 to 36 h after disease onset. A small number of mice showed unilateral hind limb paralysis without central manifestations. Animals that became moribund succumbed to the infection, while surviving mice did not show signs of disease. A dose-insensitive survival curve was observed, similar to previous findings with WNV and MVEV (12, 24, 46); thus, over a dose range of 10 to 10^5 PFU, the mortality rate was comparable (60 to 67%; Table 1). The mean survival time (MST) of animals that succumbed to infection was 12 to 13 days, except for the 10^5 PFU dose group, where a dichotic pattern of early (8 days p.i.) and late (11 days p.i.) deaths was observed, overall resulting in a shorter MST. Rapid and uniform mortality was seen when mice were infected with 10^7 PFU (MST = 6.0 days). All surviving mice infected by the s.c. route, even those infected with 10 PFU, seroconverted and showed high JEV-specific antibody ELISA endpoint titers ($\geq$3.5 log).

When mice were infected via the i.c. route, the mortality rate and average time to death were dose dependent (Table 1). Virus doses of 10 and 100 PFU gave a 100% mortality rate (MST = 8.0 and 6.4 days, respectively), while 1 PFU gave an 80% mortality rate (MST = 10.3 days) and 0.1 PFU did not result in disease. These data suggest that, in contrast to peripheral infections, the quantity of virus directly entering the brain serves as an accurate predictor of disease outcome. Consistent with the high lethality of JEV infection of the central nervous system (CNS) (a 50% lethal dose of $\leq$1 PFU given i.c.), partial seroconversion was found in the 0.1-PFU dose group.

Viral burdens in serum, spleen, spinal cord, and brain samples were determined in order to elucidate the kinetics of growth of JEV in adult B/6 mice (Fig. 1). Virus was undetectable by plaque assay in both serum and spleen samples across all time points. A more sensitive assay utilizing real-time RT-PCR detected low levels of JEV RNA in serum and spleen samples (Fig. 2). Peak viremia occurred on day 2 p.i. with a geometric mean titer (GMT) of 9×10^4 RNA copies/ml of serum, whereas splenic viral burdens peaked at day 4 p.i. with a GMT of 3×10^5 RNA copies/g of tissue. Virus invasion of the brain was first apparent on day 6 in only 3 out of 9 mice (Fig. 1). This increased to 55% of the brain samples showing virus infection at day 8 p.i. (GMT = 1×10^4 PFU) and 60% of the virus-positive brains at day 10 p.i. (GMT = 4×10^4 PFU). Viral dissemination to the spinal cord occurred later in the course of infection and was first detected on day 8 p.i. in 33% of the samples (GMT = 1×10^3 PFU), increasing to 40% of the samples collected on day 10 p.i. (GMT = 2×10^3 PFU). Accordingly, viral entry into the CNS commenced in the brain, from where the virus spread centripetally to the spinal cord.

Sections of brain tissue were examined for histopathological changes at day 10 p.i. with JEV. Hallmarks of acute viral encephalitis, including microglial nodules surrounding degenerating neurons (Fig. 3A) and perivascular leukocytic infiltration (Fig. 3B), appeared widespread in focal regions of the brain. Meningeal inflammation characterized by mononuclear infiltration of the leptomeninges was also seen (Fig. 3C). There was no evidence of demyelination, as indicated by intact myelinated axonal networks after luxol fast blue staining (Fig. 3D). Immunohistochemical staining utilizing an anti-flavivirus NS1 antibody was employed to identify specific sites of neuronal lesions within the brain parenchyma. JEV-infected neurons were found in multiple loci, predominantly localized in the cerebral cortex, hippocampus, thalamus, brain stem, and cerebellum (Fig. 3E). The pathological lesions observed served as a clinical correlate of disease.

Induction of humoral and cell-mediated immunity after JEV infection in B/6 mice. JEV-specific IgM appeared at day 4 p.i. and peaked at day 8 p.i. with a mean titer of 1:450 (Fig. 4A). Both anti-JEV IgG1 and IgG2b appeared later in the course of infection and were first detectable at 8 day p.i., attaining mean titers of 1:1,400 and 1:275, respectively, at day 10 p.i. (Fig. 4B). Qualitative measurement of the antibody response revealed neutralizing activity as early as day 4 p.i. (a 50% plaque reduction neutralization titer [$PRNT_{50}$] of 20 in 2 of 4 mice), concomitant with the onset of detectable anti-JEV IgM antibody, and reached a mean $PRNT_{50}$ of 330 (range, 80 to 640) at day 10 p.i. (Fig. 4C).

B/6 mice produced a robust $CD8^+$ T cell response following i.v. infection with 10^3 PFU JEV. The infection induced the

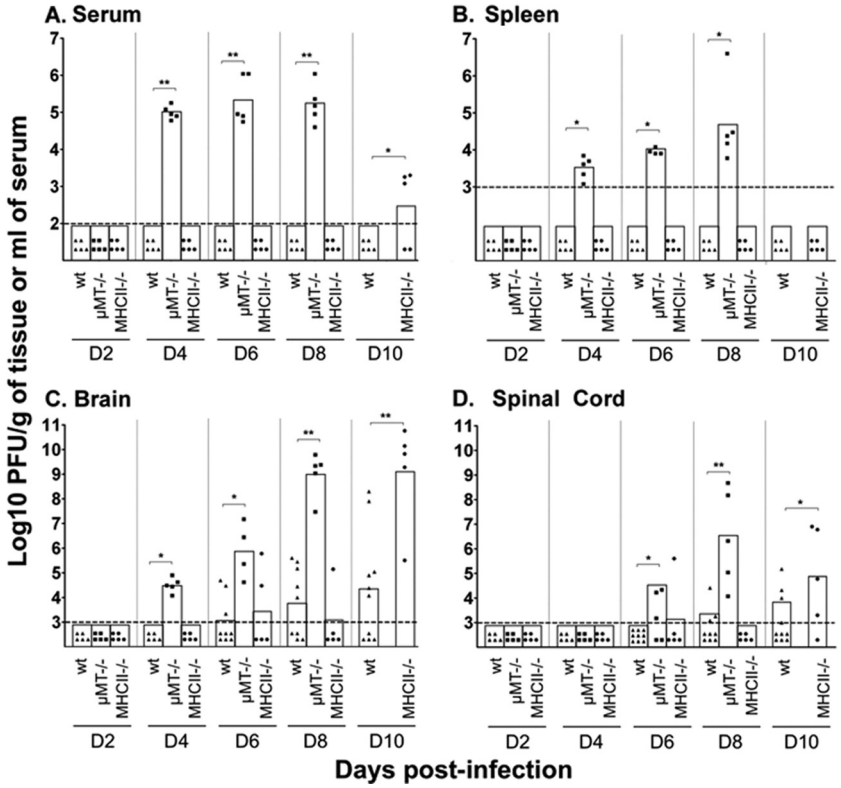

FIG. 1. JEV burdens in serum and tissue samples. JEV burdens in serum (A), spleen (B), brain (C), and spinal cord (D) samples of WT, $\mu MT^{-/-}$, and $MHCII^{-/-}$ B/6 mice after s.c. infection with 10^3 PFU of JEV are shown. At the indicated time points, animals were sacrificed and the virus contents of serum and tissue samples were measured by plaque titration. Data for WT mice were constructed from 2 independent experiments. Each symbol represents an individual mouse, and GMTs are indicated by bars. The lower limit of virus detection is indicated by the horizontal dotted line.

characteristic upregulation of expression of the early activation marker CD69, which peaked on day 1 p.i., and that of the late activation marker CD25, which peaked on day 4 p.i. (Fig. 5A). Among the $CD8^+$ T lymphocytes from JEV-primed mice, ~5% were stimulated to produce IFN-γ with JEV NS4B peptide SAVWNSTTA, also described by others to be recognized by H-$2D^b$-restricted, JEV-immune $CD8^+$ T cells (44). Another putative D^b-binding JEV peptide (on the basis of a predictive algorithm for MHC class I binding peptides using the SYFPEITHI database; reference 36) corresponding to the amino acid sequence TAWRNRELL in the E protein failed to stimulate IFN-γ production, as did a K^b-restricted ECTV-specific negative-control peptide (Fig. 5B). NS4B peptide stimulation of JEV-immune *ex vivo* splenocytes resulted in greater IFN-γ expression than stimulation with live JEV, suggesting poor efficiency of splenocyte infection and suboptimal antigen presentation with the latter approach.

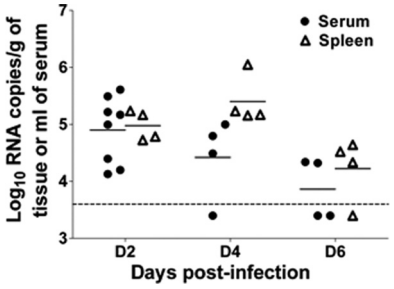

FIG. 2. JEV RNA in serum and spleen. JEV RNA detected in serum and spleen samples of B/6 WT mice after s.c. infection with 10^3 PFU of JEV are shown. At the indicated time points, animals were sacrificed and the viral RNA contents of serum and spleen samples were measured by real-time RT-PCR. Each symbol represents an individual mouse, and GMTs are indicated by horizontal bars.

The JEV-immune $CD8^+$ T cell response in the spleen, defined here by the total number of NS4B peptide-reactive $CD8^+$ lymphocytes, first appeared at day 4 p.i., reached a peak of ~10^6 cells at day 7 p.i., but markedly declined thereafter (Fig. 5C). The majority of these splenocytes were polyfunctional and expressed both IFN-γ and TNF-α following *ex vivo* stimulation with the NS4B peptide, with peak numbers of 7×10^5 cells at day 7 p.i. $CD8^+$ T cell recruitment to the site of infection was measured by isolation of lymphocytes from JEV-infected brains (Fig. 5D). $CD8^+$ T cell infiltration was already apparent at day 4 p.i., showing a 2-fold increase (1.2×10^4 cells) relative to the baseline. On day 7 p.i., corresponding to the peak of the primary JEV-specific $CD8^+$ T cell response in the spleen, $CD8^+$ T cell numbers in JEV-infected brains reached a plateau, which was maintained until at least day 10 p.i. (>100-fold increase relative to the baseline; $P = 0.002$). *Ex vivo* $CD8^+$ T cells isolated from brain at day 7 p.i. secreted IFN-γ both in the presence and in the absence of stimulation with the NS4B

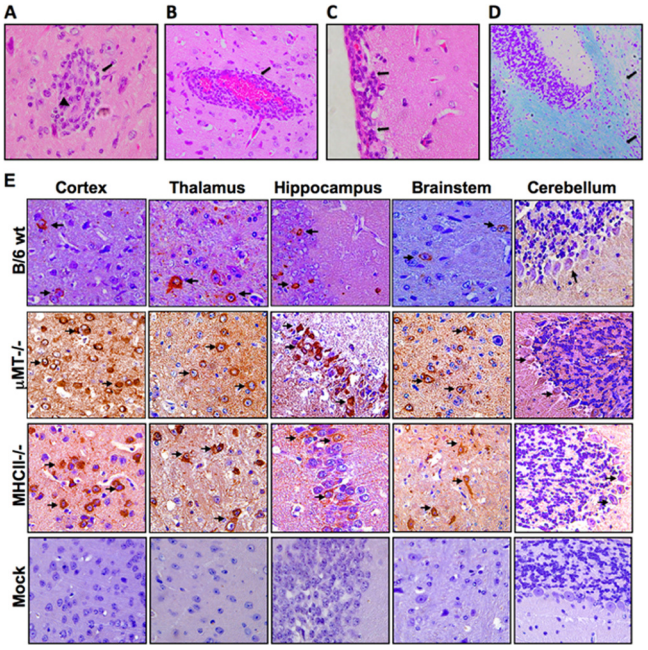

FIG. 3. Histology and immunohistochemistry analysis. Brain sections of B/6 WT mice at 10 days p.i. with 10^3 PFU of JEV s.c. are shown. Hematoxylin-and-eosin staining shows microglial nodules (arrow) with neuronophagia (arrowhead, A), perivascular mononuclear infiltration (arrow, B), and leukocytic infiltration of the meninges (arrows, C). (D) Intact myelinated axonal projections (arrows) of the cerebellum after luxol fast blue staining. (E) Detection of JEV antigen by immunohistochemistry analysis using an anti-NS1 antibody. Infected cells or injured neurons (arrows) in representative sections of the cerebral cortex, brain stem, thalamus, hippocampus, and cerebellum.

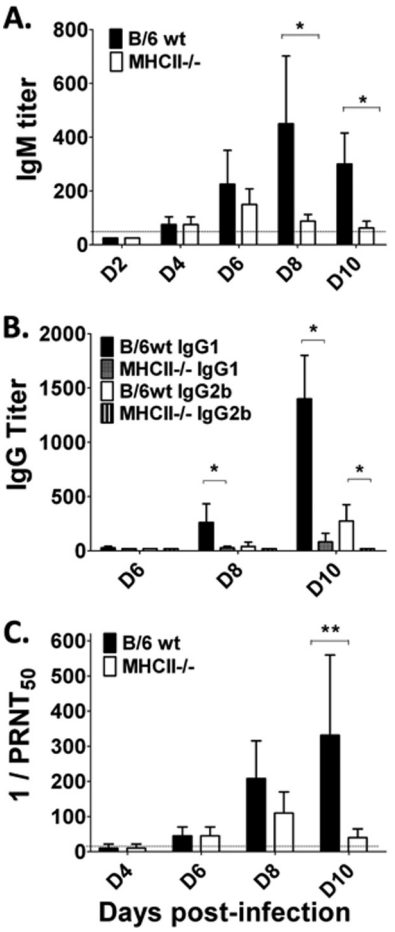

FIG. 4. Antibody responses in WT and MHCII$^{-/-}$ B/6 mice. Eight-week-old WT and MHCII$^{-/-}$ B/6 mice were infected s.c. with 10^3 PFU of JEV, and serum samples were collected at the indicated time points. Anti-JEV IgM (A) and IgG (B) isotype antibody titers were determined by ELISA. The data presented are reciprocal mean endpoint titers representative of 4 mice per group with SDs indicated by error bars. (C) Neutralizing antibody titers determined by plaque reduction neutralization assay. The data presented are mean $PRNT_{50}$s representative of 4 to 7 mice per group, and error bars indicate the SDs. Asterisks denote the significance of differences between samples from WT and MHCII$^{-/-}$ mice (*, $P < 0.05$; **, $P < 0.01$).

peptide (Fig. 5E). This is in contrast to splenocytes harvested at day 7 p.i., which required peptide stimulation for IFN-γ production. Considering the presence of virus in the brain at this time point, the difference may reflect antigen presentation via JEV-infected mononuclear cells present in brain-derived cell preparations, resulting in CD8$^+$ T cell activation and cytokine secretion in the absence of *ex vivo* peptide stimulation. Alternatively, brain-derived lymphocytes may show a greater background level of IFN-γ secretion than those isolated from the spleen.

Antibody is essential for recovery from JEV infection. To assess the role of antibody in JEV pathogenesis, mortality and virus growth following s.c. infection with 10^3 PFU of JEV were assessed in μMT$^{-/-}$ mice, which are deficient in B cells and antibody production. The challenge was uniformly lethal, and death occurred significantly earlier than in wild-type (WT) mice (MSTs = 11.1 and 12.1 days p.i., respectively; $P = 0.001$; Fig. 6). In contrast to WT mice, JEV infection produced a high level of viremia in all μMT$^{-/-}$ mice on day 4 p.i. (GMT = 1.5×10^5 PFU/ml) and the viremia persisted at that level until the animals succumbed to the infection (Fig. 1). Virus was also detected in spleen samples from infected μMT$^{-/-}$ mice at 4 days p.i. and at later time points (Fig. 1). Viral loads in brains of μMT$^{-/-}$ mice were first seen on day 4 p.i. and increased 10- and 10,000-fold at 6 and 8 days p.i., respectively, and the titers in μMT$^{-/-}$ mice exceeded those in WT mice by ~3 log and ~5 log on days 6 and 8 p.i. (Fig. 1). This is supported by histologic findings on brain sections of μMT$^{-/-}$ at day 10 p.i., revealing widespread dissemination of JEV in various brain regions, including the cerebral cortex, thalamus, hippocampus, brain stem, and cerebellum (Fig. 3E). Viral dissemination in the spinal cords of μMT$^{-/-}$ mice occurred earlier and was more widespread than in WT mice; virus was first detected on day 6 p.i. in 60% of the mice (GMT = 3×10^4 PFU) and was present in the spinal cords of all of the animals on day 8 p.i. with JEV titers exceeding those in WT mice by a 4-log margin. Taken together, the absence of antibody in μMT$^{-/-}$ mice leads to uncontrolled viremia, early neuroinvasion, widespread viral dissemination in the CNS, and a uniformly lethal outcome of infection with a shorter MST than in WT mice.

CD4$^+$ T cells are instrumental for virus clearance but not for early virus-neutralizing antibodies. MHCII$^{-/-}$ mice are

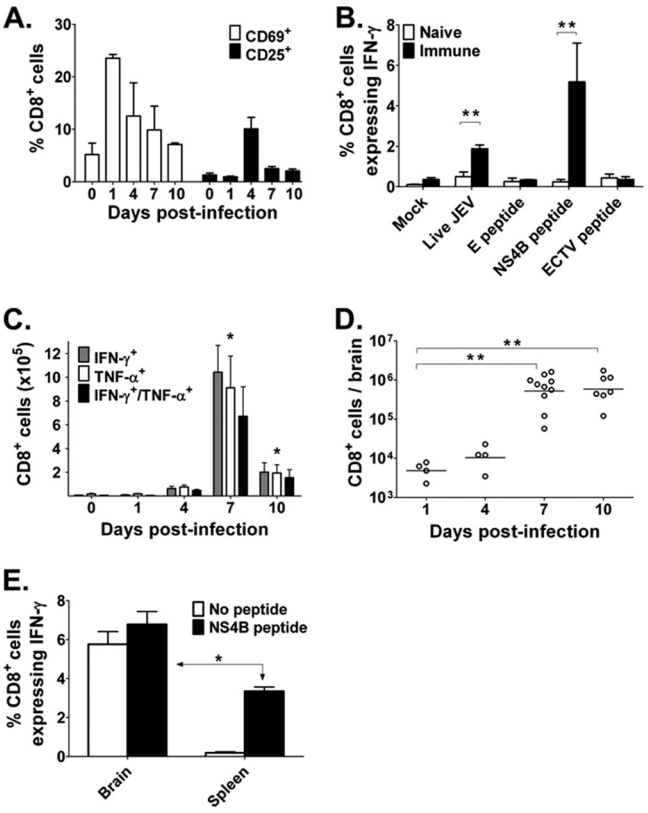

FIG. 5. $CD8^+$ T cell responses in WT B/6 mice infected with JEV. (A) Eight-week-old B/6 mice were infected i.v. with 10^3 PFU of JEV or left uninfected. Spleens ($n = 3$/group) were collected at the indicated time points, and splenocytes were stained for CD8 and the lymphocyte activation marker CD69 or CD25. The data presented are the percentages of $CD8^+$ cells expressing the early activation marker CD69 or the late activation marker CD25. Error bars denote the SDs, and data are representative of 2 independent experiments. (B) Splenocytes harvested at 7 days p.i. as described above were stimulated *ex vivo* with live JEV, D^b-restricted JEV NS4B protein- or E protein-derived peptides, a D^b-restricted or ECTV negative-control peptide or mock treated, and IFN-γ production in $CD8^+$ T cells was measured by flow cytometry. Means for 3 samples ± the SD are presented, and data are representative of 2 independent experiments. (C) Kinetics of JEV-immune $CD8^+$ T cell activation measured after *ex vivo* stimulation with D^b-restricted JEV NS4B peptide. Data show the number of $CD8^+$ T cells/spleen that express IFN-γ, TNF-α, or both cytokines following stimulation. Means for 3 samples ± the SDs are presented, and data are representative of 2 independent experiments. (D) Kinetics of $CD8^+$ cell infiltration of the brains of 8-week-old WT B/6 mice infected s.c. with 10^3 PFU of JEV. Lymphocytes were isolated from the brains of infected mice as described in Materials and Methods and stained for CD8 expression. Each symbol represents an individual mouse, and a horizontal line indicates the mean value for each time point. (E) JEV-immune $CD8^+$ T cells in spleens and brains of B/6 WT mice infected s.c. with 10^3 PFU of JEV at 7 days p.i. were measured by IFN-γ expression in $CD8^+$ cells following *ex vivo* stimulation in the presence or absence of JEV NS4B peptide. Means for 6 to 8 samples ± the SDs are presented. Asterisks denote significant differences (*, $P < 0.05$; **, $P < 0.01$).

deficient in $CD4^+$ T cells, which are, in turn, important in priming and memory formation of antiviral B and $CD8^+$ T cell responses and the production of inflammatory cytokines (49). All $MHCII^{-/-}$ mice succumbed to JEV infection, in contrast to the mortality rate of 55% of a group of age-matched WT

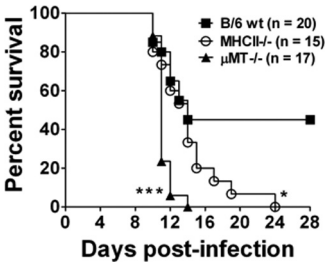

FIG. 6. Susceptibility of WT, $\mu MT^{-/-}$, and $MHCII^{-/-}$ B/6 mice to infection with JEV. Groups of 12-week-old mice were infected s.c. with 10^3 PFU of JEV. Morbidity and mortality were recorded daily, and surviving mice were monitored for 28 days. The data shown were constructed from two independent experiments. The significance of differences in mortality between WT and knockout mice was determined by using the log-rank test (*, $P = 0.028$; ***, $P = 0.0002$).

mice ($P = 0.028$; Fig. 6). Interestingly, the MST of infected $MHCII^{-/-}$ mice suggested a dual course of disease progression, where the MST of the majority of mice was similar to that of WT controls (~12.5 days p.i.), while 21% of $MHCII^{-/-}$ mice displayed a longer average time to death (~20 days p.i.). Similar to that in WT mice, virus was not detectable by plaque assay in serum and spleen samples during the first 8 days of infection and virus was found in brain samples of some mice at 6 and 8 days p.i. (Fig. 1). However, at 10 days p.i., 3 out of 5 $MHCII^{-/-}$ mice developed a moderate viremia and all animals showed virus in the brain with the GMT exceeding that of WT controls by a 4-log margin. Histologic examination revealed widespread dissemination of JEV in the brains of $MHCII^{-/-}$ mice at day 10 p.i. (Fig. 3E). Virus dissemination in the spinal cord was also more prominent in $MHCII^{-/-}$ than WT mice at 10 days p.i. (Fig. 1).

The lack of $CD4^+$ T cells did not prevent the induction of a JEV-specific IgM response in infected $MHCII^{-/-}$ mice but markedly truncated this response (Fig. 4A). While peaking at day 8 p.i. in WT mice, JEV-specific IgM declined after day 6 p.i. in $MHCII^{-/-}$ mice and was significantly lower on days 8 and 10 p.i. than in WT mice ($P = 0.02$). Immunoglobulin class switching to IgG was significantly blunted in $MHCII^{-/-}$ mice, with anti-JEV IgG1 titers in WT mice exceeding those in the $CD4^+$ T cell-deficient mice by ~10- and 20-fold on days 8 and 10 p.i., respectively (Fig. 3B). IgG2b isotype antibodies against JEV first appeared at 10 days p.i. in WT mice but remained undetectable in $MHCII^{-/-}$ mice (Fig. 4B). Importantly, the neutralizing activity of the humoral immune response against JEV first detectable in both mouse strains at day 6 p.i. increased only marginally on day 8 p.i. in infected $MHCII^{-/-}$ mice and subsequently declined, while in WT mice, neutralizing antibody levels continued to increase. As a consequence, the $PRNT_{50}$ in JEV-infected WT mice (mean, 330; range, 80 to 640) significantly exceeded that in $MHCII^{-/-}$ mice (mean, 40; range, 20 to 80) at day 10 p.i. ($P = 0.007$; Fig. 4C). Accordingly, the deficient humoral immune response after day 6 p.i. in $MHCII^{-/-}$ mice most likely is the dominant factor contributing to the late viremia and high mortality rate in the JEV-infected host lacking $CD4^+$ T cell function.

Marginal contribution of $CD8^+$ T cells to the control of JEV infection. To establish the role of $CD8^+$ T cells in recovery from primary JEV infection, B/6 mice were depleted of $CD8^+$

TABLE 2. Effect of CD8$^+$ T cell depletion on susceptibility of B/6 and 129 mice to JEV infection

Mouse strain and treatment[a]	% Deaths (no. of deaths/total [P value])[b]	MST (days) ± SD (P value)[c]
B/6		
Isotype control	67 (14/21)	13.0 ± 1.7
CD8$^+$ T cell depleted	84 (16/19 [0.07])	12.1 ± 2.6 (0.12)
129 × 1/SvJAPB		
Isotype control	11 (1/9)	14
CD8$^+$ T cell depleted	0 (0/11 [0.26])	

[a] Eight-week-old mice were treated i.p. with 0.5 mg of CD8$^+$ T cell-depleting or isotype control antibody in 500 μl PBS on days −1, 0, +1, and +7 of a s.c. challenge with 10^3 PFU of JEV. Surviving mice were monitored for 28 days.
[b] Survival data were analyzed for significant differences between the treated and corresponding control groups by the log-rank test. The data shown were constructed from two independent experiments.
[c] Differences in MSTs between treated and control groups were analyzed for significance by the Mann-Whitney test.

TABLE 3. Contributions of humoral and cellular immune responses to recovery from JEV infection

Treatment (no. of cells)[a]	% Deaths (no. of deaths/total [P value])[b]	MST (days) ± SD[c]
PBS control	70 (7/10)	12.0 ± 2.0
Naïve splenocytes (1×10^7)	73 (22/30)	12.5 ± 2.0
Immune splenocytes (1×10^7)	0 (0/10 [0.0004])	
Immune B cells (5×10^6)	0 (0/10 [0.0004])	
Immune T cells (5×10^6)	29 (6/21 [0.0017])	12.8 ± 1.0
Immune CD4$^+$ T cells (5×10^6)	64 (9/14 [0.99])	12.1 ± 2.0
Immune CD8$^+$ T cells (5×10^6)	76 (16/21 [0.59])	12.0 ± 2.3

[a] Eight-week-old donor B/6 mice were infected i.v. with 10^3 PFU of JEV or left uninfected and sacrificed 7 days later for splenocyte collection and purification of splenocyte subpopulations. Cells were transferred to 8-week-old B/6 mice, and recipients were infected s.c. with 10^3 PFU of JEV a day later. Surviving mice were monitored for 28 days.
[b] Data are representative of 2 independent experiments. Immune splenocyte treatment groups were compared to the naïve splenocyte control group to test for statistically significant differences.
[c] No significant difference between immune splenocyte treatment and control groups was noted.

T cells *in vivo* and challenged with 10^3 PFU JEV s.c. (Table 2). An only marginal, and statistically insignificant, increase in susceptibility to JEV was seen compared to that of a group of B/6 mice treated with an isotype control antibody (84% and 67% mortality rates, $P = 0.07$). Similarly, the time to death was slightly shorter in CD8$^+$ T cell-depleted mice than in the control group ($P = 0.12$; Table 2). CD8$^+$ T cell depletion did not allow the generation of detectable viremia by plaque assay during the course of JEV infection (data not shown). In addition, serum and spleen viral loads at day 10 p.i. did not differ between CD8$^+$ T cell-depleted and mock-treated mice infected with JEV (Fig. 7A). However, CD8$^+$ T cells contributed to a significant degree to reduced virus growth in the brain and spinal cord (Fig. 7B). Thus, depletion of CD8$^+$ T cells resulted in an ~100-fold increase in virus titers in both tissues on day 10 p.i., relative to those of controls, accompanied by a greater number of spinal cord samples showing the presence of virus in treated relative to mock-treated animals. Thus, although CD8$^+$ T cells did not provide a significant advantage in terms of survival following JEV infection, they demonstrated a beneficial role in controlling virus growth in the CNS, with the proviso that the latter may occur at the cost of increased immunopathology.

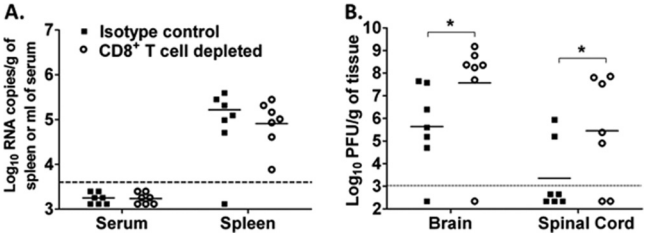

FIG. 7. *In vivo* depletion of CD8$^+$ T cells increases viral burdens in the brain and spinal cord. Groups of CD8$^+$ T cell-depleted and control antibody-treated 8-week-old WT B/6 mice were infected s.c. with 10^3 PFU of JEV and sacrificed on day 10 p.i. to determine the viral loads in the serum and spleen by real-time RT-PCR and those in the brain and spinal cord by plaque titration. Symbols represent individual mice, and data were constructed from two independent experiments. The horizontal line denotes the GMT. An asterisk denotes a significant difference ($P < 0.05$).

Since the already high susceptibility of B/6 mice to JEV infection may have concealed a survival advantage mediated by CD8$^+$ T cells in the depletion experiment, we tested the contribution of CD8$^+$ T cells to recovery from JEV infection in the 129 mouse strain, which shows a low mortality rate (~10%) following s.c. infection with 10^3 PFU of JEV. The depletion of CD8$^+$ T cells had no impact on the survival rate of JEV-infected 129 mice (Table 2).

The protective effect of JEV-immune T cells requires both the CD4$^+$ and CD8$^+$ subpopulations. Infection of B/6 mice with JEV elicits a vigorous cellular immune response, which is illustrated by the protective value of JEV-immune splenocyte transfer in recipient mice against a JEV challenge (Table 3). Thus, total immune splenocytes and purified B cells protected all recipient mice against s.c. infection with 10^3 PFU JEV when transferred 1 day before a challenge. However, transfer of purified JEV-immune CD4$^+$ or CD8$^+$ T cells did not provide a significant survival advantage to recipient mice challenged with JEV (Table 3). Interestingly, pooled transfer of both T cell subpopulations significantly reduced the mortality rate in a group of recipient mice ($P = 0.002$; Table 3). These data yet again show the dominant protective role of the humoral immune response contrasting with an at best marginal contribution of CD8$^+$ T cells in recovery from primary infection with JEV.

Deficiencies in the cytolytic effector pathways of lymphocytes do not exacerbate the pathogenesis of JEV. CD8$^+$ T cells exhibit direct antiviral activity by killing virus-infected cells via two cytolytic effector mechanisms, the Fas-mediated death pathway and the granule exocytosis pathway, involving the delivery of perforin and granzymes into the target cell. Having already demonstrated that neither *in vivo* depletion nor transfer of virus-immune CD8$^+$ T cells significantly impacted the disease outcome, we predicted that mice defective in Fas, perforin, or granzymes A and B would show a susceptibility to JEV similar to that of WT mice. Indeed, neither the mortality rate nor the MST differed significantly between WT and Fas$^{-/-}$, perf$^{-/-}$, or gzmA/B$^{-/-}$ mice tested at 8 and 12 weeks of age (Fig. 8A and B, respectively). In contrast, CNS viral

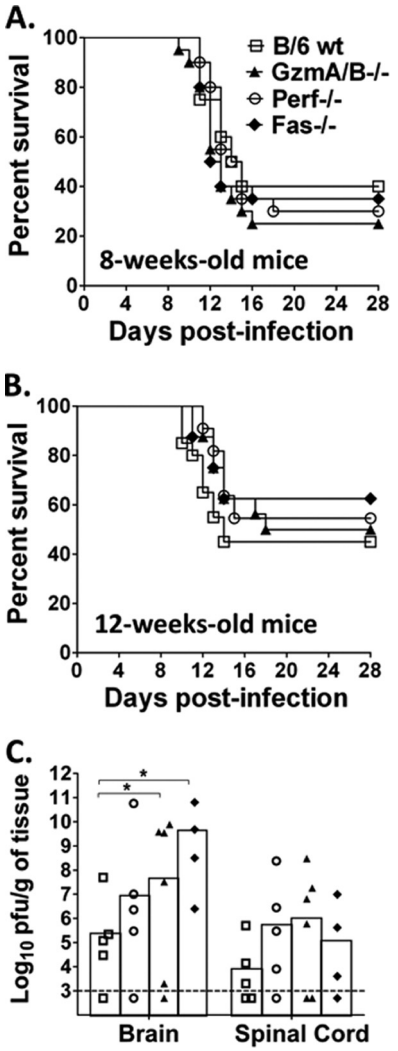

FIG. 8. Susceptibility of mice defective in cytolytic effector pathways to infection with JEV. Groups of 8-week-old (A) and 12-week-old (B) WT, perf$^{-/-}$, gzmA/B$^{-/-}$, and Fas$^{-/-}$ B/6 mice were challenged s.c. with 10^3 PFU of JEV and monitored for death for 28 days. The data shown were constructed from 3 independent experiments. (C) Viral loads in the brains and spinal cords of 8-week-old WT and knockout mice infected s.c. with 10^3 PFU of JEV were measured by plaque titration. Symbols represent individual mice, and bars denote GMTs. An asterisk denotes a significant difference ($P < 0.05$).

burdens at day 10 p.i. in perf$^{-/-}$, Fas$^{-/-}$, and gzmA/B$^{-/-}$ mice were elevated compared to those of WT mice and the difference reached significance in brain samples from the latter two strains (Fig. 8C).

DISCUSSION

B/6 mice showed a partial susceptibility to s.c. infection via the footpad with the prototype strain of JEV, and ~60% of the animals developed a lethal encephalitis over a wide dose range of 10 to 10^5 PFU. This lack of a dose response in the mortality rate following a virus challenge by an extraneural route is a hallmark of flavivirus infection (for instance, see references 12 and 24) and is thought to reflect, at least in part, induction of more vigorous innate immune responses critical in early control of virus dissemination with increasing amounts of virus used for infection (30). Consistent with high-dose WNV and MVEV infections in B/6 mice (24, 46), s.c. injection of 10^7 PFU of JEV was uniformly lethal and the MST corresponded to that of groups of mice i.c. inoculated with 10^2 PFU of JEV. This finding and that of the presence of multiple loci of infection in the brain support the hematogenous route as the principal pathway of JEV entry into the CNS and imply that the virus content of blood is a key determinant thereof. Vero cell-grown JEV was used exclusively in this investigation. Interestingly, studies with cell culture have suggested that flavivirus propagated in mosquito cells could differentially modulate innate immune responses from virus grown in mammalian cells (2, 40). However, this conclusion was not supported by pathogenesis studies with mice (11, 25).

The humoral immune response was critically important for the recovery of mice from an extraneural challenge with JEV. Mice lacking B cells and the ability to produce antibody (μMT$^{-/-}$ mice) developed a high level of viremia at day 4 p.i. which persisted until all of the animals succumbed to infection; early entry of virus into the brain with widespread dissemination in the CNS was also found. Additionally, purified immune B cell transfer fully protected recipient WT mice from a JEV challenge. The appearance of viremia and splenic tissue viral titers at day 4 p.i. in μMT$^{-/-}$ mice correlated with the time point when antibodies with neutralizing activity became detectable in JEV-infected WT mice. Antibodies elicited against flaviviruses clear the virus by neutralization of infectivity or indirectly by antibody-dependent cell-mediated cytotoxicity, Fc-γ receptor-mediated clearance, or complement-mediated cytotoxicity (34). Thus, in mice lacking the ability to clear the viruses by antibody, JEV and WNV (8, 12) cause a fulminating and lethal infection.

T cell help was not required to mount an early IgM response against JEV; however, the response was truncated in MHCII$^{-/-}$ relative to that in WT mice. As expected, IgG class switching, first observed in WT mice at ~8 days p.i., was markedly blunted in the absence of CD4$^+$ T cells. This dysfunctional antibody response largely explains the adverse outcome of JEV infection in MHCII$^{-/-}$ mice, which was characterized by a uniform mortality rate, elevated brain viral titers, and viral dissemination in the spinal cord. Moreover, 60% of MHCII$^{-/-}$ mice displayed detectable viremia late in the course of infection, when a significant disparity in neutralizing antibody titers in WT and MHCII$^{-/-}$ mice was found. Failure of effective virus clearance from extraneural tissues most likely accounted for CNS invasion in all infected MHCII$^{-/-}$ mice and, as a consequence, a 100% mortality rate. Some JEV-infected MHCII$^{-/-}$ mice showed a markedly protracted time to death, which could have been the result of either delayed entry into the CNS following the late viremia associated with waning neutralizing antibody or reduced lymphocyte infiltration of the infected brain associated with reduced immunopathological manifestations. A study of the role of CD4$^+$ T cells in WNV infection also found a truncation of IgM and blunting of IgG antibody responses due to the absence of CD4$^+$ T cells, as well as a uniform mortality rate with prolonged survival of some mice (42). Accordingly, the protective role of CD4$^+$ T cells by providing help for antibody responses is clearly apparent in

both flavivirus models. However, a second critical function of $CD4^+$ T cells, their requirement for a sustained $CD8^+$ T cell response and, consequently, $CD8^+$ T cell-mediated clearance of virus from the CNS documented for WNV (42) was not apparent in the mouse model for Japanese encephalitis, given the failure of $CD8^+$ T cells to effectively clear JEV from the CNS and prevent a lethal disease outcome.

A striking finding of this study was the lack of effect of $CD8^+$ T cells on the survival phenotype in the mouse model of Japanese encephalitis. We confirmed that infection of B/6 mice with JEV elicited functional, virus-specific, $CD8^+$ T cells, illustrated by the production of IFN-γ and TNF-α upon *ex vivo* stimulation of lymphocytes with a previously described H-$2D^b$ JEV NS4B peptide (44). This response was comparable in magnitude to that elicited by WNV against the corresponding WNV NS4B peptide (5, 35) and followed the commonly found kinetics of induction of anti-flavivirus cytotoxic T cells, with peak activity in the spleen at day 7 p.i. (17, 35). We also confirmed a high level of $CD8^+$ T cell infiltration of the brain in response to JEV infection. Thus, given the effective induction and functionality of anti-JEV $CD8^+$ T cells, it was surprising that transfer of this JEV-immune splenocyte population failed to provide protection against JEV in recipient mice. Similarly, *in vivo* depletion of >98% of the $CD8^+$ T cells in two mouse strains (B/6 and 129) that differ in susceptibility to JEV did not markedly impact the mortality rate following a JEV challenge. Furthermore, genetic deficiency in key molecules (Fas, perforin, or granzymes A and B) of the two main $CD8^+$ T cell cytolytic effector pathways did not alter the susceptibility of B/6 mice to JEV. However, the viral burden in the CNS was significantly higher in $CD8^+$ T cell-depleted mice and mice defective in cytolytic effector pathways than in control mice, showing *in vivo* functionality of the response. It remains unclear whether immunopathology associated with $CD8^+$ T cell infiltration of the brain or an insufficient magnitude of the response, *per se*, explains why the viral load reduction in the CNS mediated by $CD8^+$ T cells did not translate into a survival advantage. Collectively, these data suggest an at best marginal contribution of $CD8^+$ T cells to recovery from infection with JEV.

This and other investigations of the immunobiology of the encephalitic flaviviruses have uncovered a conflicting role for $CD8^+$ T cells in recovery from infection. While the $CD8^+$ T cell response is essential for virus elimination from the CNS and survival in mouse models of West Nile encephalitis (38, 39, 46, 47) and a disease-potentiating effect of cytotoxic T cells was documented in mice infected with MVEV (24), we show here that in JEV, the $CD8^+$ T cell response does not markedly affect the outcome of the infection. Notably, mice genetically deficient in the Fas- or perforin-dependent pathway of cytotoxicity showed greatly increased susceptibility to virulent lineage I WNV infection (37) but did not differ from WT mice in susceptibility to infection with JEV (Fig. 8) or lineage II WNV strain Sarafend (47) and were more resistant to infection with MVEV (24). These findings highlight a difference in pathogenesis between closely related flaviviruses belonging to the JEV serocomplex that most likely involves a difference in the capacity of the cellular immune response to resolve the virus infections in the CNS. It has been well documented that extraneural infection of adult mice with virulent lineage I WNV produces virus titers in the brain of 10^3 to 10^5 PFU in the majority of the animals between days 6 and 10 p.i. and that $CD8^+$ T cell-mediated clearance of virus from the CNS allows most of the mice to recover (for instance, see references 38 and 39). Similar immune system-mediated resolution of virus infection of the CNS leading to an improved disease outcome is not apparent in murine infections with JEV and MVEV, where a strong correlation between the CNS infection rate and the mortality rate exists (this study and reference 24). The mouse models of West Nile virus, Murray Valley encephalitis virus, and JEV infections may reflect the human diseases caused by these viruses, given that patients with WNV meningitis and encephalitis often have less severe outcomes (26) than patients with Japanese or Australian encephalitis, who frequently suffer long-term debilitating neurological complications (7, 43).

REFERENCES

1. **Adachi, M., et al.** 1995. Targeted mutation in the Fas gene causes hyperplasia in peripheral lymphoid organs and liver. Nat. Genet. **11:**294–300.
2. **Arjona, A., et al.** 2007. West Nile virus envelope protein inhibits dsRNA-induced innate immune responses. J. Immunol. **179:**8403–8409.
3. **Beasley, D. W., P. Lewthwaite, and T. Solomon.** 2008. Current use and development of vaccines for Japanese encephalitis. Expert Opin. Biol. Ther. **8:**95–106.
4. **Biswas, S. M., V. M. Ayachit, G. N. Sapkal, S. A. Mahamuni, and M. M. Gore.** 2009. Japanese encephalitis virus produces a CD4+ Th2 response and associated immunoprotection in an adoptive-transfer murine model. J. Gen. Virol. **90:**818–826.
5. **Brien, J. D., J. L. Uhrlaub, and J. Nikolich-Zugich.** 2007. Protective capacity and epitope specificity of CD8(+) T cells responding to lethal West Nile virus infection. Eur. J. Immunol. **37:**1855–1863.
6. **Burke, D. S., et al.** 1985. Fatal outcome in Japanese encephalitis. Am. J. Trop. Med. Hyg. **34:**1203–1210.
7. **Burrow, J. N., et al.** 1998. Australian encephalitis in the Northern Territory: clinical and epidemiological features, 1987-1996. Aust. N.Z. J. Med. **28:**590–596.
8. **Chambers, T. J., et al.** 2008. West Nile 25A virus infection of B-cell-deficient ((micro)MT) mice: characterization of neuroinvasiveness and pseudoreversion of the viral envelope protein. J. Gen. Virol. **89:**627–635.
9. **Clark, D. C., et al.** 2007. In situ reactions of monoclonal antibodies with a viable mutant of Murray Valley encephalitis virus reveal an absence of dimeric NS1 protein. J. Gen. Virol. **88:**1175–1183.
10. **Colombage, G., R. Hall, M. Pavy, and M. Lobigs.** 1998. DNA-based and alphavirus-vectored immunisation with prM and E proteins elicits long-lived and protective immunity against the flavivirus, Murray Valley encephalitis virus. Virology **250:**151–163.
11. **Daffis, S., M. A. Samuel, M. S. Suthar, M. Gale, Jr., and M. S. Diamond.** 2008. Toll-like receptor 3 has a protective role against West Nile virus infection. J. Virol. **82:**10349–10358.
12. **Diamond, M. S., B. Shrestha, A. Marri, D. Mahan, and M. Engle.** 2003. B cells and antibody play critical roles in the immediate defense of disseminated infection by West Nile encephalitis virus. J. Virol. **77:**2578–2586.
13. **Goncalvez, A. P., et al.** 2008. Humanized monoclonal antibodies derived from chimpanzee Fabs protect against Japanese encephalitis virus in vitro and in vivo. J. Virol. **82:**7009–7021.
14. **Gupta, A. K., V. J. Lad, and A. A. Koshy.** 2003. Protection of mice against experimental Japanese encephalitis virus infections by neutralizing anti-glycoprotein E monoclonal antibodies. Acta Virol. **47:**141–145.
15. **Halstead, S. B., and J. Jacobson.** 2003. Japanese encephalitis. Adv. Virus Res. **61:**103–138.
16. **Kägi, D., et al.** 1994. Cytotoxicity mediated by T cells and natural killer cells is greatly impaired in perforin-deficient mice. Nature **369:**31–37.
17. **Kesson, A. M., R. V. Blanden, and A. Müllbacher.** 1987. The primary in vivo murine cytotoxic T cell response to the flavivirus, West Nile. J. Gen. Virol. **68**(Pt. 7)**:**2001–2006.
18. **Kimura-Kuroda, J., and K. Yasui.** 1988. Protection of mice against Japanese encephalitis virus by passive administration with monoclonal antibodies. J. Immunol. **141:**3606–3610.
19. **Kitamura, D., and K. Rajewsky.** 1992. Targeted disruption of mu chain membrane exon causes loss of heavy-chain allelic exclusion. Nature **356:**154–156.
20. **Klein, R. S., and M. S. Diamond.** 2008. Immunological headgear: antiviral immune responses protect against neuroinvasive West Nile virus. Trends Mol. Med. **14:**286–294.
21. **Lee, E., R. A. Hall, and M. Lobigs.** 2004. Common E protein determinants

for attenuation of glycosaminoglycan-binding variants of Japanese encephalitis and West Nile viruses. J. Virol. **78:**8271–8280.
22. **Lee, E., and M. Lobigs.** 2002. Mechanism of virulence attenuation of GAG-binding variants of Japanese encephalitis and Murray Valley encephalitis viruses. J. Virol. **76:**4901–4911.
23. **Libraty, D. H., et al.** 2002. Clinical and immunological risk factors for severe disease in Japanese encephalitis. Trans. R. Soc. Trop. Med. Hyg. **96:**173–178.
24. **Licon Luna, R. M., et al.** 2002. Lack of both Fas ligand and perforin protects from flavivirus-mediated encephalitis in mice. J. Virol. **76:**3202–3211.
25. **Lim, P. Y., K. L. Louie, L. M. Styer, P. Y. Shi, and K. A. Bernard.** 2010. Viral pathogenesis in mice is similar for West Nile virus derived from mosquito and mammalian cells. Virology **400:**93–103.
26. **Lindsey, N. P., J. E. Staples, J. A. Lehman, and M. Fischer.** 2010. Surveillance for human West Nile virus disease—United States, 1999-2008. MMWR Surveill. Summ. **59:**1–17.
27. **Lobigs, M., et al.** 2010. An inactivated Vero cell-grown Japanese encephalitis vaccine formulated with Advax, a novel inulin-based adjuvant, induces protective neutralizing antibody against homologous and heterologous flaviviruses. J. Gen. Virol. **91:**1407–1417.
28. **Mackenzie, J. S., D. J. Gubler, and L. R. Petersen.** 2004. Emerging flaviviruses: the spread and resurgence of Japanese encephalitis, West Nile and dengue viruses. Nat. Med. **10:**S98–S109.
29. **Madsen, L., et al.** 1999. Mice lacking all conventional MHC class II genes. Proc. Natl. Acad. Sci. U. S. A. **96:**10338–10343.
30. **Monath, T. P., et al.** 2003. Chimeric live, attenuated vaccine against Japanese encephalitis (ChimeriVax-JE): phase 2 clinical trials for safety and immunogenicity, effect of vaccine dose and schedule, and memory response to challenge with inactivated Japanese encephalitis antigen. J. Infect. Dis. **188:**1213–1230.
31. **Müllbacher, A., M. Lobigs, and E. Lee.** 2003. Immunobiology of mosquito-borne encephalitic flaviviruses. Adv. Virus Res. **60:**87–120.
32. **Müllbacher, A., et al.** 2004. Can we really learn from model pathogens? Trends Immunol. **25:**524–528.
33. **Murali-Krishna, K., V. Ravi, and R. Manjunath.** 1996. Protection of adult but not newborn mice against lethal intracerebral challenge with Japanese encephalitis virus by adoptively transferred virus-specific cytotoxic T lymphocytes: requirement for L3T4+ T cells. J. Gen. Virol. **77:**705–714.
34. **Pierson, T. C., D. H. Fremont, R. J. Kuhn, and M. S. Diamond.** 2008. Structural insights into the mechanisms of antibody-mediated neutralization of flavivirus infection: implications for vaccine development. Cell Host Microbe **4:**229–238.
35. **Purtha, W. E., et al.** 2007. Antigen-specific cytotoxic T lymphocytes protect against lethal West Nile virus encephalitis. Eur. J. Immunol. **37:**1845–1854.
36. **Rammensee, H., J. Bachmann, N. P. Emmerich, O. A. Bachor, and S. Stevanovic.** 1999. SYFPEITHI: database for MHC ligands and peptide motifs. Immunogenetics **50:**213–219.
37. **Shrestha, B., and M. S. Diamond.** 2007. Fas ligand interactions contribute to CD8+ T-cell-mediated control of West Nile virus infection in the central nervous system. J. Virol. **81:**11749–11757.
38. **Shrestha, B., and M. S. Diamond.** 2004. Role of CD8+ T cells in control of West Nile virus infection. J. Virol. **78:**8312–8321.
39. **Shrestha, B., M. A. Samuel, and M. S. Diamond.** 2006. CD8+ T cells require perforin to clear West Nile virus from infected neurons. J. Virol. **80:**119–129.
40. **Silva, M. C., A. Guerrero-Plata, F. D. Gilfoy, R. P. Garofalo, and P. W. Mason.** 2007. Differential activation of human monocyte-derived and plasmacytoid dendritic cells by West Nile virus generated in different host cells. J. Virol. **81:**13640–13648.
41. **Simon, M. M., et al.** 1997. In vitro- and ex vivo-derived cytolytic leukocytes from granzyme A x B double knockout mice are defective in granule-mediated apoptosis but not lysis of target cells. J. Exp. Med. **186:**1781–1786.
42. **Sitati, E. M., and M. S. Diamond.** 2006. CD4+ T-cell responses are required for clearance of West Nile virus from the central nervous system. J. Virol. **80:**12060–12069.
43. **Solomon, T.** 2004. Flavivirus encephalitis. N. Engl. J. Med. **351:**370–378.
44. **Trobaugh, D. W., L. Yang, F. A. Ennis, and S. Green.** 2010. Altered effector functions of virus-specific and virus cross-reactive CD8+ T cells in mice immunized with related flaviviruses. Eur. J. Immunol. **40:**1315–1327.
45. **Tscharke, D. C., et al.** 2005. Identification of poxvirus CD8+ T cell determinants to enable rational design and characterization of smallpox vaccines. J. Exp. Med. **201:**95–104.
46. **Wang, Y., M. Lobigs, E. Lee, and A. Müllbacher.** 2003. CD8+ T cells mediate recovery and immunopathology in West Nile virus encephalitis. J. Virol. **77:**13323–13334.
47. **Wang, Y., M. Lobigs, E. Lee, and A. Müllbacher.** 2004. Exocytosis and Fas mediated cytolytic mechanisms exert protection from West Nile virus induced encephalitis in mice. Immunol. Cell Biol. **82:**170–173.
48. **Zhang, M. J., M. J. Wang, S. Z. Jiang, and W. Y. Ma.** 1989. Passive protection of mice, goats, and monkeys against Japanese encephalitis with monoclonal antibodies. J. Med. Virol. **29:**133–138.
49. **Zhu, J., H. Yamane, and W. E. Paul.** 2010. Differentiation of effector CD4 T cell populations. Annu. Rev. Immunol. **28:**445–489.